XAFS of $Ga_{1-x}Mn_xAs$ Alloys

A. M. Stuckey, M. Boyanov, T. Shibata, T. Wojtowicz,
Y. Sasaki, X. Liu, J. Furdyna, B. A. Bunker
University of Notre Dame, Notre Dame, IN, U.S.A.

Introduction

Dilute magnetic semiconductors (DMSs) have been an area of interest in solid-state physics because of the combination of magnetism and semiconductor technology [1]. This coupling opens the possibility of spin-based mechanisms for devices, as well as the ability to tune the band offset of the semiconductor via magnetic fields. Initial work focused on II-Mn-VI alloys; however, these materials have not been found suitable for the creation of semiconductor devices with ferromagnetic properties at room temperature.

A large part of the difficulty concerning the II-VI-based magnetic semiconductors is that the magnetism of the alloy depends on the concentration of the magnetic ions in the semiconductor, and increasing the concentration of magnetic ions increases antiferromagnetic behavior rather than ferromagnetic behavior [2]. On the other hand, III-Mn-V materials have been shown to behave ferromagnetically to much higher temperatures via a hole-mediated ordering of the Mn spins [3, 4]. Early studies of III-V Mn alloys — specifically $Ga_{1-x}Mn_xAs$ — have shown that the Mn enters the III-V lattice on the cation site, creating a p-type alloy for low Mn concentrations [5]. In attempts to increase the Curie temperature by increasing the Mn concentration, the Mn entered other sites within the lattice as the concentration increased. In this study, fluorescence XAFS measurements of these manganese DMS materials have been performed to study the Mn site as grown and after annealment.

Methods and Materials

Fluorescence x-ray absorption fine structure (XAFS) studies were carried out at the Materials Research Collaborative Access Team (MR-CAT) 10-ID beamline at the APS. This beamline is equipped with a cryogenic double-crystal Si(111) monochromator and tunable undulator that allows XAFS measurements over an energy range from 5 to more than 30 keV. A harmonic rejection mirror was used to eliminate the third and higher x-ray harmonics from the monochromator. The x-ray beam was defined to a vertical width of 2 mm and a horizontal width of 150 μm at 6.5 keV (slightly less than the K absorption edge of Mn). Helium-filled flight paths were used to transmit the x-ray beam through the hutch to decrease the loss of photons due to air absorption. Elastic scattering due to the highly crystalline nature of the GaAs substrates upon which the samples were grown necessitated the use of a 13-element solid-state detector. The solid-state detector was able to differentiate between the elastically scattered photons and the fluorescence photons.

The samples for this study were $Ga_{1-x}Mn_xAs$ grown on a GaAs substrate, with $x = 0.08$. The samples were positioned so that the incident x-ray beam struck the sample at a grazing angle, such that the penetration depth of the x-rays was only slightly larger than the thickness of the $Ga_{1-x}Mn_xAs$ layer. XAFS measurements were collected for an as-grown sample, an "optimally annealed" sample, and an "overannealed" sample. The descriptions "optimal" and "over" refer to the Curie temperature of the samples; the optimal sample exhibited the greatest Curie temperature, and the overannealed sample was annealed to a temperature such that the Curie temperature was below the optimal value.

Results

Initial studies have been undertaken with fluorescence measurements, as shown in Fig. 1. The differences between the samples are difficult to see when examining the normalized spectra. The data then have the smoothly varying atomic background removed, and the result is then Fourier transformed. The magnitudes of the Fourier transforms (FTRs) of the data are shown in Fig. 2. The overannealed sample, with a double peak, is quite different from the as-grown and optimally annealed samples. Both the optimally annealed and the as-grown

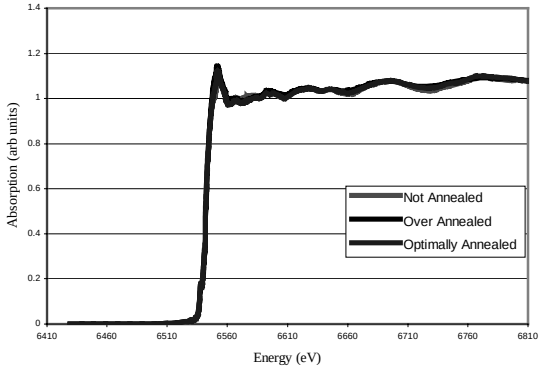

FIG. 1. Absorption spectra for the sample 10823Eb series: as grown, overannealed, and optimally annealed.

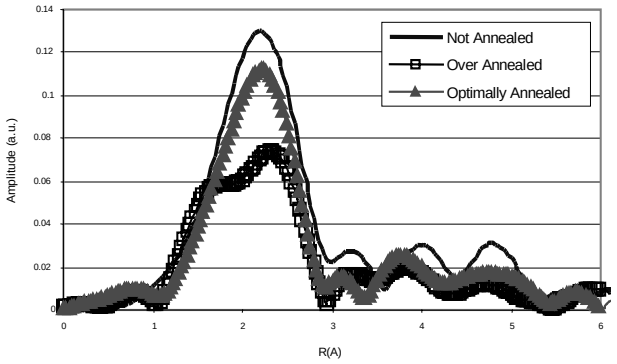

FIG. 2. Fourier transform magnitudes for the $Ga_{1-x}Mn_xAs$ materials: as grown, optimally annealed, and overannealed.

samples exhibit similar nearest neighbor peaks; however, in shells of larger distance, the differences between these two are much more apparent.

The real and imaginary parts of the Fourier transform, from which the magnitude is derived, are then fit by using a number of theoretical calculations and comparison with known standards.

Discussion

The measurements for this project were made at the end of the year, and the analysis is still ongoing. Several possibilities for the smaller-radius peak in the overannealed sample are being examined, and we hope to have a more definitive answer soon from examining more samples.

Acknowledgments

This work was supported in part by the U.S. Department of Defense, Defense Advanced Research Projects Agency (DARPA) SpinS Program through the State University of New York. Work performed at MR-CAT was supported by funding from the U.S. Department of Energy (DOE) under Grant No. DEFG0200ER45811 and by the member institutions. Use of the Advanced Photon Source was supported by the DOE Office of Science, Office of Basic Energy Sciences, under Contract No. W-31-109-ENG-38

References

[1] H. Ohno, A. Shen, F. Matsukura, A. Oiwa, A. Endo, S. Katsumoto, and Y. Iye, Appl. Phys. Lett. **69**, 363 (1996).

[2] *Optical Properties of Semiconductor Nanostructures*, edited by M. L. Sadowski et al. (Kluwer Academic Publishers, Netherlands, 2000), p. 211.

[3] Dietl, A. Haury, and Y. Merle d'Aubigné, Phys. Rev. B **55**, R3347 (1997).

[4] F. Matsukura, H. Ohno, A. Shen, and Y. Sugawara, Phys. Rev. B **57**, R2037 (1998).

[5] R. Shioda, K. Ando, T. Hayaski, and M. Tanaka, Phys. Rev. B **58**, 1100 (1998).